Journal of the European Ceramic Society **16** (1996) 1121–1126

PII: S0955-2219(96)00026-X
0955-2219/96/$15.00

Low-Temperature Oxidation of Silicon Nitride by Water in Supercritical Condition

Edoardo Proverbio[a] & Fabio Carassiti[b]

[a]University of Rome 'La Sapienza', Department ICMMPM, via Eudossiana 18, 00184 Roma, Italy
[b]Third University of Rome, Department of Mechanics and Automation, via Segre 60, 00146 Roma, Italy

(Received 28 April 1995; revised version received 10 January 1996; accepted 12 January 1996)

Abstract

Oxidation tests carried out in supercritical water (400–500°C) revealed a noticeable corrosion attack on the silicon nitride surface in spite of the low temperatures. Increasing water pressure generally caused an increase in the oxidation phenomena. Oxidation scale evolution depended strictly on the silicon nitride sintering process, sintering aids, porosity and impurities, which influenced oxidation kinetics and surface morphology. In such test conditions the solubility of silica in water seemed to have a great influence on the stability of the oxidation scale, mainly in reaction-bonded silicon nitride samples. © 1996 Elsevier Science Limited.

1 Introduction

The most promising properties of silicon nitride, from the viewpoint of extensive applications such as thermal barriers and antiwear coatings, are hardness and chemical stability, these resulting from strong covalent bonds. Silicon nitride may also find applications in high-temperature environments as combustion engines, burners and high-temperature gas heat exchangers, while other applications include low-temperature high-water-pressure environments such as steam generators, nuclear reactors or chemical plants.

However, like all non-oxide ceramics (SiC, B_4C, AlN, BN), silicon nitride is inherently unstable in an oxidizing atmosphere, and water too can act as an oxidizing agent either at low or high temperature.[1] The influence of water vapour at high temperatures (1000–1500°C) on the oxidation of Si_3N_4 was described about 20 years ago,[2,3] but it is only recently that more accurate investigations have been carried out. Singhal[3] reported that the activation energy for oxidation of silicon nitride is 488 ± 30 kJ mol^{-1} in wet oxygen and 375 ± 25 kJ mol^{-1} in dry oxygen. Such an influence could result from the diffusion and dissolution of OH^- ions through the surface oxide film. More recently, Opila[4] reported some results on the oxidation kinetics of chemically vapour deposited SiC in wet oxygen. The oxidation rates of SiC in oxygen containing 10% water vapour were only very slightly enhanced over the rates found in dry oxygen, the obtained activation energies were 41 and 142 kJ mol^{-1}, respectively. The influence of water on corrosion kinetics was strongly enhanced by the presence of alkali impurities. Oxidation tests carried out in a high-purity Al_2O_3 tube (80–200 ppm Na_2O), instead of a quartz tube, led to an activation energy of 249 kJ mol^{-1} in oxygen containing 10% water vapour. According to Opila the water vapour plays a role in the transport of sodium and aluminium from the reaction tube to the sample surface, since contamination did not occur when experiments were performed with the Al_2O_3 reaction tube in dry oxygen. The impurities, as well as water[3,5,6], increase the crystallization rate of silica and enhance the transformation of crystobalite to tridymite.[7] Thus, the impurity effects should not be isolated from the oxidation rate enhancement due to water vapour. Devitrification and phase transformation promote the formation of cracks and fissures, thus exposing new, free Si_3N_4 for oxidation. Roughening of the surface by bubbles and pits was also observed[5] on the oxidized silicon nitride surface.

Since the oxidation resistance of Si_3N_4 depends on the formation of protective SiO_2, it should be supposed the material can suffer from corrosive phenomena under high water pressure even at low temperatures. It was reported[8–10] that the solubility of silica in water is strongly dependent on pressure and temperature, amorphous silica being about an order of magnitude more soluble than crystalline silica.

Yoshimura and co-workers[11–14] have studied the oxidation mechanisms of Si_3N_4 and SiC under hydrothermal conditions from 10 to 100 MPa, at temperature as low as 200 or 600°C: oxidation yielded amorphous silica scales (a hydrosilica sol was proposed instead by Hirayama *et al.*[15]) and

NH_3, and CH_4, CO, CO_2 and H_2, respectively. Under 10 MPa, Si_3N_4 yielded $N_2 + H_2$ instead of NH_3. In a wear test condition at 300°C and 8·53 MPa water pressure, C_2H_6 gas was also detected in the SiC/H_2O system.[16] In the same system the formation of carbon layers was observed and investigated.[13,14,17] The oxidation kinetics of silicon nitride follow the parabolic law, but at high temperature (>800°C) it seems that the oxidation rate was unaffected by water vapour pressure above 1·5 MPa, as reported by Sato *et al.*[18]

Sintered Si_3N_4 with and without sintering aids has been studied at 300°C and 8·6 MPa by Yoshio and Oda.[19] Corrosion damage of doped Si_3N_4 was characterized by pit formation with the development of different shapes, depending on the sintering aids used. The pit size and population, and the formation of pit agglomerate, depended on the duration of exposure to the aggressive environment. On the other hand, the corrosion behaviour of Si_3N_4 without additives was characterized by intergranular attack due to selective dissolution of the SiO_2 phase at grain boundaries.[20] As the grain boundaries dissolve, the Si_3N_4 grains are undermined and fall into the solution, hence accelerating corrosion.

In the present study, a series of oxidation tests was carried out in the range 14–40 MPa in the water supercritical region (temperature >400°C) on different types of silicon nitride in order to evaluate the influence of sintering process and environment aggressiveness on the corrosion resistance of silicon nitride.

2 Experimental Procedure

Two kinds of oxidation tests were performed: a short-time exposure at different water pressures and different temperatures to determine the influence of such parameters on corrosion phenomena, and a time-dependent exposure at fixed pressure and temperature to provide a rough evaluation of the oxidation kinetics.

2.1 Materials

Hot-pressed (HPSN; Cercom Coors Inc., USA), sintered reaction-bonded (SRBSN; Nitrasil S, AED Ltd, UK) and reaction-bonded (RBSN; Nitrasil R, AED Ltd, UK) commercially available silicon nitride samples were used in these experiments. Before testing samples were characterized chemically and physically. Grain size was revealed by microscope observation after chemical etch (5 min in molten KOH). Open porosity was measured by means of an intrusion mercury porosimeter. Results are summarized in Table 1.

Crystalline phase and elementary composition were determined by means of X-ray diffraction, using Cu K_α radiation filtered by a LiF monochromator and an EDS electron microprobe, respectively. Results are reported in Table 2.

For the first test sequence, one of the larger surfaces of the sample to be tested (4 × 10 × 4 mm) was ground to 1 μm finish with diamond paste. For the second test sequence, some coupons (10 × 10 × 1 mm) were obtained by cutting the as-received sample with a diamond saw. Surfaces were then ground with a 16 μm diamond wheel.

2.2 Oxidation

Oxidation tests were carried out in a closed Nimonic 105 autoclave heated by means of a heater strip. After being cleaned ultrasonically in acetone, the samples were placed in a platinum crucible with the polished surface upwards. A second platinum crucible, containing the calculated amount of distilled water to reach the scheduled pressure, was then placed above the previous one. Eight different oxidation tests were performed in total, as summarized in Table 3.

For the time-dependent oxidation test, a minimum of four coupons was used for each type of silicon nitride; after being carefully weighed with a precision balance, these specimens were placed in different platinum crucibles. Tests were performed for 5, 40 and 100 h at 400°C and 36 MPa. After cooling down the autoclave, samples were dried and re-weighed.

2.3 Characterization of oxidized samples

Oxidized samples were characterized by means of three different techniques. Morphological characterization was performed by scanning electron microscopy (SEM). Information on the composition of the oxidation scale was obtained by Fourier transform infra-red spectroscopy (FTIR), which provided information on the amorphous phase in the outer oxidation layer, and also by X-ray diffraction (XRD). FTIR analysis was carried out on bulk samples using a single-beam diffuse reflectance

Table 1. Microstructural parameters of samples

Sample	*Density (g cm^{-3})*	*Avrg. grain length (μm)*	*Avrg. grain diameter (μm)*	*Open porosity (% vol)*	*Avrg. pore diameter (μm)*
HPSN	3·31	6	1	0·07	6·1
SRBSN	3·22	10	2·5	0·16	2·0
RBSN	2·60	–	–	21·96	0·1

Table 2. Sample composition as determined from X-ray diffraction patterns and EDS microanalysis

Sample	*Main phase*	*Main secondary phase*	*Sintering aids and impurities content (wt% as oxide)*			
			Y_2O_3	Al_2O_3	Fe_2O_3	CaO
HPSN	β-Si_3N_4	$Y_5N(SiO_4)_3$	9·7	1·8	0·3	–
SRBSN	β-Si_3N_4	–	1·5	3·2	–	–
RBSN	α-Si_3N_4 (60%)	β-Si_3N_4 (40%)	–	0·6	0·2	0·2

Table 3. Temperature and pressure for each oxidation test (duration = 24 h in each case)

Test	*Temperature (°C)*	*Pressure (MPa)*
A	400	12
B	400	22
C	400	30
D	400	40
IA	500	14
IB	500	20
IC	500	30
ID	500	40

configuration in the spectral range from 1400 to 200 cm^{-1} with a resolution of 2 cm^{-1}. A silvered mirror was used for background measurement.

3 Results

The first oxidation test sequence was carried out to evaluate the influence of temperature and pressure on the oxidation process, keeping the soaking time constant, to try to elucidate the different behaviour of the samples. In fact, by comparing the results obtained at the same operating condition, it was possible to evaluate differences in oxidation behaviour as a function of the silicon nitride formation technology.

With the second oxidation test it was possible to obtain a rough estimate of the kinetics of the oxidation process itself. However, results are only indicative because the weight changes during the process were influenced by many mechanisms, sometimes being in contrast with each other. Some of them led to a weight loss, others to a weight gain.

3.1 RBSN oxidation

Reaction-bonded silicon nitride is composed almost exclusively of a mixture of α-Si_3N_4 and β-Si_3N_4 with some impurities. So the oxidation process is conditioned by the direct reaction of silicon nitride with the external environment and by porosity. After the low-pressure test (14 MPa at 400 and 500°C) the morphology of the sample surface remained almost unchanged. However, the FTIR spectra showed a slight increase of the intensity of the peak corresponding to the Si–O stretching vibrational mode (1105 cm^{-1}), and a decrease of the Si–N stretching vibrational mode (Si–Nbs) due to the β-Si_3N_4 molecule (959 cm^{-1}) was noticed. In the diffraction patterns a broad peak positioned around the SiO_2 reflection (amorphous silica) was found; a sharp peak of low intensity due to the trydimite reflection was also detected.

In the test carried out at 20 MPa, the RBSN behaviour was little influenced by temperature. However, the amount of silicon nitride β-phase on the surface was reduced, as evidenced by FTIR analysis. Such an observation confirms that the β-phase is preferentially oxidized with respect to the α-phase, similar results have been reported by Contet *et al.*[11] for silicon nitride powder after hydrothermal oxidation. In the supercritical region oxidation is more marked (Fig. 1). The surface silica content increases and the presence of calcium silicate (probably rankiite) becomes evident (round particles in Fig. 2).

The time-dependent test (Fig. 3) showed that RBSN exhibited a weight increase at intermediate times (40 h), whereas after long exposure (100 h) the sample underwent a dramatic weight reduction. The strong initial weight gain may be explained by initial internal oxidation of the pores, which follows parabolic kinetics. The SiO_2 film grew on the pore walls, eventually closing the pores. After this the oxidation rate decreased, the weight increment being due only to external oxide growth.[21] The subsequent weight loss could be due to dissolution of the silica in the supercritical water, following linear kinetics.

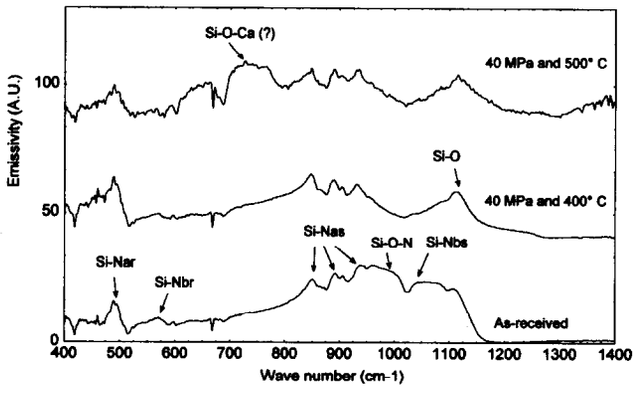

Fig. 1. FTIR spectra of RBSN samples after oxidation tests. Si–Nbs, beta-silicon nitride stretching vibrational mode, Si–Nbr, beta-silicon nitride rocking vibrational mode; Si–Nas, alpha-silicon nitride stretching vibrational mode; Si–Nar, alpha-silicon nitride rocking vibrational mode.

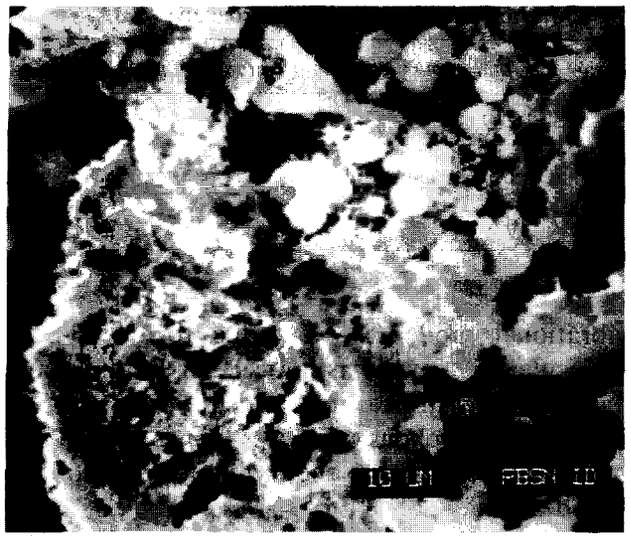

Fig. 2. SEM micrograph of RBSN sample after oxidation tests at 500°C and 40 MPa water pressure.

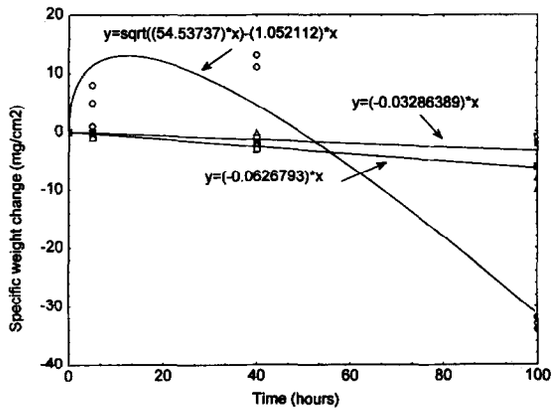

Fig. 3. Weight change vs. time for RBSN (○), HPSN (□) and SRBSN (△) samples after exposure at 400°C and 36 MPa water pressure.

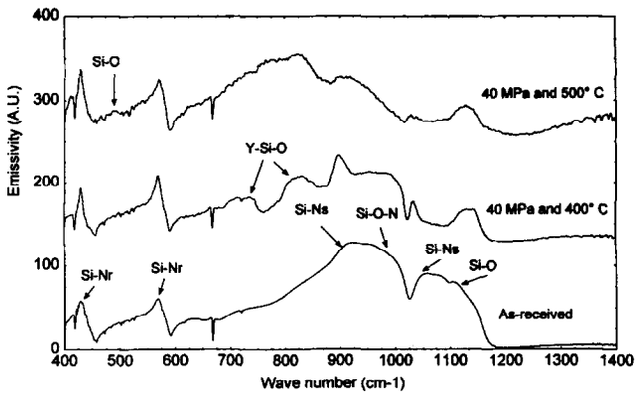

Fig. 4. FTIR spectra of HPSN samples after oxidation tests. Si–Ns, beta-silicon nitride stretching vibrational mode; Si–Nr, beta silicon nitride rocking vibrational mode.

Fig. 5. SEM micrograph of HPSN sample after oxidation tests at 400°C and 30 MPa water pressure.

3.2 HPSN oxidation

The oxidation resistance of hot-pressed silicon nitrides is conditioned strictly by the presence of sintering aids. In the low-temperature low-pressure test, the surface was practically unaffected by oxidation phenomena. On increasing the temperature, a noticeable amount of silica associated with a reduction of the stretching vibrational mode peak of silicon nitride was observed in FTIR spectra (Fig. 4). At higher pressure, but in the subcritical region, the surface was damaged markedly. Surface roughening was due to intense silica formation (strongly marked at 500°C) and was coupled with a reduction of the Si–O–N reflection in the FTIR spectra (960 cm^{-1}).

At 30 MPa and 400°C there was a noticeable increase in the content of yttrium silicon oxynitries ($Y_2ON_4Si_{12}O_{48}$ crystal and vitreous phase) as clearly shown in Fig. 5. Greater differences than in the subcritical region were revealed in the corresponding high-temperature test. In fact, at 500°C the above glassy phase disappeared as also confirmed by X-ray diffraction analysis. Such phenomena could be explained by detachment of the incoherent glassy phase itself due to its excessive growth. At the maximum pressure reached such a situation was more evident.

As far as the oxidation kinetics are concerned, the time-dependent test revealed a continuous, but limited, weight loss (Fig. 3).

3.3 SRBSN oxidation

The oxidation mechanism of sintered reaction-bonded silicon nitride was similar to that observed for HPSN. At low temperature the formation of a superficial glassy phase was observed. At 40 MPa this layer became incoherent and detached easily, exposing a silica-rich substrate (Fig. 6). Very interesting results were observed for tests conducted at 500°C: the nucleation and progressive growth of $Y_2Si_2O_5$ yttrium silicate crystals (Fig. 7). The growth of such crystals was strongly influenced by the water pressure, being maximized at 40 MPa. FTIR analysis revealed the almost complete disappearance

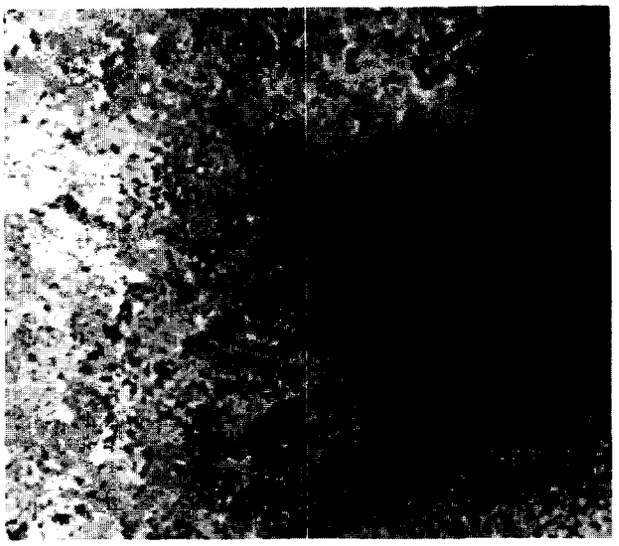

Fig. 6. SEM micrograph of SRBSN sample after oxidation tests at 400°C and 40 MPa water pressure.

Fig. 7. SEM micrograph of SRBSN sample after oxidation tests at 500°C and 40 MPa water pressure. The arrows indicate yttrium silicate crystals.

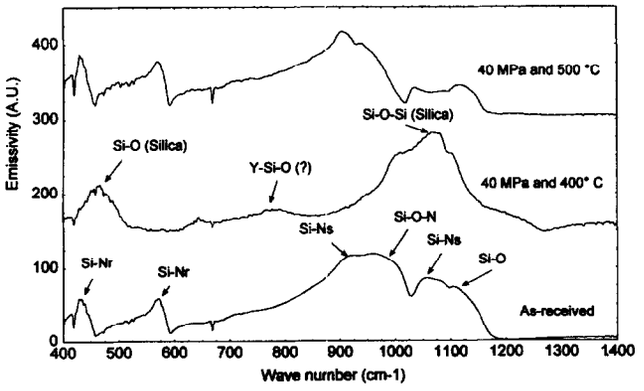

Fig. 8. FTIR spectra of SRBSN samples after oxidation tests. Si–Ns, beta-silicon nitride stretching vibrational mode; Si–Nr, beta-silicon nitride rocking vibrational mode.

of Si–O–N and Si–O–Si (silica) peaks (Fig. 8). The oxidation kinetics also showed a behaviour similar to that observed for HPSN with a weight loss increasing with time, but in this case a little more marked.

4 Discussion

Different considerations have to be made in the case of silicon nitride samples containing sintering aids and those comprising almost pure reaction-bonded silicon nitride. In the former case the growth of a silica glassy phase rich in metal ions is predominant. This is followed by debonding of such layers, exposing the underlying silica-rich scale, and thus increasing the environment aggressiveness. In the case of HPSN and SRBSN the oxidation reactions lead to a weight decrease with time. The loss of material in gas form (N_2, H_2 or NH_3), due to dissolution in supercritical water, and due to mechanical debonding of the incoherent scale, is predominant. Assuming linear kinetics for the weight loss, an apparent linear rate constant of 0·033 and 0·063 mg cm^{-2} h^{-1} was calculated for HPSN and SRBSN, respectively (Table 4).

A situation which should be discussed separately is the oxidation process at 500°C of SRBSN. In this case the nucleation and growth of yttrium silicate crystals over the oxidation scale were observed. Such phenomena could be related to the hydrothermal growth of crystals.[22] The different amount of sintering aids (and probably of minor contaminants), leading to a different composition, solubility and viscosity of the glassy phase, may explain the lack of a similar process for HPSN samples. However, further tests are required for a fuller explanation.

In the case of RBSN, internal oxidation due to its high open porosity characterizes the first oxidation stage with a noticeable weight gain.[21] The solubility of silica in supercritical water, following linear kinetics, could be the main factor influencing the weight loss observed after 100 h exposure at 400°C and 36 MPa. Such an assertion is supported also by visual observations: after cooling down the autoclave, there was a white deposit (silica powder) all over the platinum crucible and autoclave walls. Coupling the two processes, the

Table 4. Parabolic rate constant k_p (mg^2 cm^{-4} h^{-1}) and linear rate constant k_l (mg cm^{-2} h^{-1}) calculated from experimental data

Sample type	k_p	k_l
HPSN	–	0·033
RBSN	54·53	1·052
SRBSN	–	0·063
Silica glass[10]	–	0·176

effective weight changes of RBSN should follow the relationship

$$\frac{dw}{dt} = \frac{k_p}{t} - k_l$$

where w is the specific weight change (mg cm^{-2}), k_p the parabolic rate constant (mg^2 cm^{-4} h^{-1}) and k_l the linear rate constant (mg cm^{-2} h^{-1}). Fitting the experimental data (Fig. 3) by using the quasi-Newton estimation method and a least-squares loss function with the parametric function

$$w = \sqrt{k_p t} - k_l t$$

yielded an apparent parabolic oxidation rate constant (k_p) of 54·53 mg^2 cm^{-4} h^{-1} and an apparent linear weight loss rate constant k_l of 1·05 mg cm^{-2} h^{-1}. This last value is about six times higher than that reported by Ito and Tomozawa,[10] 0·176 mg cm^{-2} h^{-1}, for silica glass (a density of 2·2 g cm^{-3} was assumed here) in distilled water at 285°C under 100 MPa pressure. For comparison, the corresponding values of the constants for HPSN and SRBSN are reported in Table 4.

At high water pressure, independent of the temperature, the oxidation scale is characterized by enrichment in ion impurities, mainly calcium, which lead to the formation of incoherent oxidation product. The selective oxidation of the β-silicon nitride phase was evidenced by FTIR spectra. This preferential oxidation could however be an artefact, since if the β-phase origin is a film over the α-grains,[11] its consumption will undoubtedly be faster and predominant over the α-phase. Such assumptions have yet to be demonstrated.

5 Conclusions

(1) In spite of the low temperature, high-pressure water oxidation tests significantly alter the surface of sintered silicon nitride. Increasing both pressure and temperature causes the oxidation attack to be stronger and stronger.

(2) In such situations sintering aids and impurities also have a detrimental effect on oxidation behaviour, promoting the formation of incoherent glassy phase over the surface in analogy with the high-temperature (1000°C) oxidation mechanism.

(3) The high open porosity has a strong influence on the oxidation kinetics of RBSN. A noticeable weight gain was observed after 40 h exposure at 400°C and 36 MPa.

(4) The solubility of silica in supercritical water seems to have a great influence on the stability of the oxidation scale, mainly on the RBSN sample surface.

References

1. Gogotsi, Y. G. & Yoshimura, M., Water effect on corrosion behaviour of structural ceramics. *MRS Bull.*, **19**[10] (1994) 39–54.
2. Horton, R. M., Oxidation kinetics of powdered silicon nitride. *J. Am. Ceram. Soc.*, **52**[3] (1969) 121–124.
3. Singhal, S. C., Effect of water vapor on the oxidation of hot pressed silicon nitride and silicon carbide. *J. Am. Ceram. Soc.*, **59**[1–2] (1976) 81–82.
4. Opila, E. J., Oxidation kinetics of chemically vapor-deposited silicon carbide in wet oxygen. *J. Am. Ceram. Soc.*, **77**[3] (1994) 730–736.
5. Maeda, M., Nakamura, K. & Ohkubo, T., Oxidation of silicon nitride in a wet atmosphere. *J. Mater. Sci. Lett.*, **24** (1989) 2120–2126.
6. Proverbio, E., Rossi, D. & Cigna, R., Influence of water vapour on high-temperature oxidation of Al_2O_3–MgO doped hot-pressed silicon nitride. *J. Eur. Ceram. Soc.*, **9** (1992) 453–458.
7. Opila, E. J., Influence of alumina reaction tube impurities on the oxidation of chemically vapor-deposited silicon carbide. *J. Am. Ceram. Soc.*, **78**[4] (1995) 1107–1110.
8. Kennedy, G., A portion of the system silica–water. *Econ. Geol.*, **45**[7] (1950) 629–653.
9. Iler, R. K., *The Chemistry of Silica*. John Wiley & Sons, Inc., New York, 1979.
10. Ito, S. & Tomozawa, M., Stress corrosion of silica glass. *J. Am. Ceram. Soc.*, **64** (1981) C-60.
11. Contet, C., Kase, J. I., Noma, T. & Yoshimura, M., Hydrothermal oxidation of Si_3N_4 powder. *J. Mater. Sci. Lett.*, **6** (1987) 963–964.
12. Yoshimura, M., Kase, J. I., Hayakawa, M. & Somiya S., Oxidation mechanism of nitride and carbide powders by high-temperature, high-pressure water. *Ceram. Trans.*, **10** (1990) 337–354.
13. Gogotsi, Y. G. & Yoshimura, M., Low-temperature oxidation, hydrothermal corrosion, and their effects on properties of SiC (Tyranno) fibers. *J. Am. Ceram. Soc.*, **78**[6] (1995) 1439–1450.
14. Gogotsi, Y. G. & Yoshimura, M., Degradation of SiC (Tyranno) fibers in high-temperature, high-pressure water. *J. Mater. Sci. Lett.*, **14** (1995) 755–759.
15. Hirayama, H., Kawakubo, T., Goto, A. & Kaneko, T., Corrosion behaviour of silicon carbide. *J. Am. Ceram. Soc.*, **72**[11] (1989) 2049–2053.
16. Kitaoka, S., Tsuji, T., Katoh, T., Yamaguchi, Y. & Kashiwagi, K., Tribological characteristics of SiC ceramics in high-temperature and high-pressure water. *J. Am. Ceram. Soc.*, **77**[7] (1994) 1851–1856.
17. Gogotsi, Y. G., Kofstad, P., Yoshimura, M. & Nickel, K., Formation of sp^3-bonded carbon upon hydrothermal treatment of SiC. *Diamond Relat. Mater.*, (in press).
18. Sato, T., Haryu, K., Endo, T. & Shimada M., High temperature oxidation of silicon nitride-based ceramics by water vapour. *J. Mater. Sci.*, **22** (1987) 2635–2640.
19. Yoshio, T. & Oda, K., Aqueous corrosion and pit formation of Si_3N_4 under hydrothermal conditions. *Ceram. Trans.*, **10** (1990) 367–385.
20. Oda, K., Yoshio, T., Miyamoto, Y. & Koizumi, M., Hydrothermal corrosion of pure, hot isostatically pressed silicon nitride. *J. Am. Ceram. Soc.*, **76**[5] (1993) 1365–1368.
21. Thümmler, P. F., Oxidation mechanism of porous silicon nitride. *J. Mater. Sci. Lett.*, **19** (1984) 1283–1295.
22. Somiya, S., Yoshimura, M., Suzuki, & M. L. Yamaguchi, T., Mullite powder from hydrothermal processing. *Ceram. Trans.*, **6** (1990) 287–310.